A Visible Spectral Atlas of Geostationary Satellites

Adam Battle, Vishnu Reddy, Roberto Furfaro, Tanner Campbell
University of Arizona, USA
James Frith, David Monet
Air Force Research Laboratory, USA

ABSTRACT

The Robotic Automated Pointing Telescope for Optical Reflectance Spectroscopy (RAPTORS) is an automated 0.6-meter, f/4.6 telescope constructed by five engineering students at the University of Arizona. The telescope is fitted with a transmission grating with a spectral resolution of R~30 in the visible wavelength range (0.45 – 0.95 microns), resulting in a roughly 15 nm resolution. This system has allowed us to conduct the initial phase of a slitless spectroscopic survey for over 60 GEO-belt satellites. Observations were conducted with a cadence of at least one spectrum per minute, producing an average of ~800 spectra per night. Data calibration included flats once per lunation, CCD dark- and bias-frames each night, and nightly spectra of a G2V solar analog star for solar reflectance calibration. Although empirical results have shown that a single solar analog is sufficient for visible reflectance measurements, additional airmass correction stars were also observed most nights to better account for atmospheric extinction effects if needed. Initial results from the survey show that visible spectroscopy is a powerful tool for satellite characterization and discrimination.

We present examples of an individual satellite's 3-dimensional Spectral Phase Map (SPM) of longitudinal phase angle vs. wavelength vs. normalized reflectance (out-of-plane axis). In addition to the spectral data, the zeroth order of the images can be used to produce uncalibrated, panchromatic lightcurves for more traditional satellite characterization methods. Comparisons between the SPM and zeroth order lightcurves show good correlation between traditional glint features and the features in phase-wavelength space. Additional "flux-neutral" color features are also identifiable which maintain the satellite's brightness in the lightcurve but change the reflectance at certain wavelengths. Complementary to the phase-wavelength maps, full-night median spectra are presented as a tool for target characterization and discrimination. Initial results show a strong correlation between satellite bus-type and the median spectrum's shape across multiple satellites. This is promising for the prospect of creating a bus-type based GEO spectral taxonomy. These results show that the GEO spectral survey meets its goals of providing methods to discriminate targets via lightcurve data and Spectral Phase Maps as well as for fingerprinting individual satellites. It is possible that these spectral data represent the foundations for a GEO satellite taxonomy, which exceeds the expectations of this survey.

Due to the promising nature of the initial results of this survey, ongoing observational efforts are focusing on a subset of targets that will be representative of their bus type. Four bus types were chosen for an in-depth analysis with three satellites in each bus type. Satellites were chosen such that constituents of a given group are separated by no more than 15 degrees in orbital longitude to limit viewing geometry effects on the study. Each of the selected targets will be observed once per month over a year to investigate seasonal variations in the full-night median spectra. Target observations will be clustered by bus type to reduce night-to-night seasonal variations within the bus group. Potential future work could include machine learning techniques on SPMs for object discrimination and bus-type identification, spectral modeling for material composition extraction, increased spectral coverage, or expansion of the survey to other longitudes in the U.S.

1. INTRODUCTION

Observations are crucial for resident space object (RSO) tracking and orbit determination as well as the characterization of an RSO's physical properties. References [1-5] have shown that low-resolution reflectance spectroscopy can be used to successfully identify a small subset of materials on RSOs [6]. A proof of concept for the Rapid Automated Pointing Telescope for Optical Reflectance Spectroscopy (RAPTORS I) hyperspectral survey of the GEO belt was demonstrated in [6]. This survey has since begun and preliminary results are described here that show low-resolution spectroscopy is a powerful technique for characterizing, differentiating, and identifying geostationary Earth orbit (GEO) satellites. The current most common form of GEO characterization employs

telescopic observations of a target to obtain photometric brightness measurements throughout a night as the longitudinal phase angle varies (e.g. [7]). The addition of a transmission diffraction grating in the place of one of these photometric filters allows higher spectral resolution (~15 nm wide) bands to be collected simultaneously with a zeroth order, panchromatic measurement.

2. OBSERVATIONS

The RAPTORS I telescope is located on the campus of the University of Arizona and is a 0.610 m, f/4.64 Newtonian reflector. The telescope is equipped with a Finger Lakes Instrumentation Proline 4710 CCD and a filter wheel with a 30-line mm^{-1} transmission diffraction grating allowing us to obtain slitless spectroscopy. The resulting system has a field of view of 16 arcminutes on a side with a plate scale of 0.9 arcsec px^{-1} and a spectral resolution of 14.6 nm px^{-1} in the wavelength range of 450 – 950 nm (R~30). The wavelength calibration was initially estimated using the grating equation for telescope plate scale [8] and was refined by observing the H-α emission line from Seifert galaxy M106. Observations of asteroid (3) Hebe were used to verify the wavelength resolution by comparing RAPTORS I results with published results from NASA's Planetary Data System archive [9].

Observations were obtained by tracking at the GEO's rate – which is small, but non-zero – to maintain the object in center of the telescope's field of view. Exposures were taken at a cadence of roughly one image per minute. Trusted G2V or equivalent solar analog stars were observed once per night to calibrate the GEO spectra into reflectance measurements. The most commonly used solar analogs were HD 129357, SAO 120107, and SAO 93936. Once per night, on the opposite end of the night as the solar analog, a standard star was also observed as it passed close to the target GEO's position. These standard stars were collected each night to be used for additional atmospheric corrections if needed. Dark and bias frames were acquired nightly and flat frames for the grating were obtained once per lunation. CCD image reduction was performed using MaxIm DL (Cyanogen Imaging) and standard reduction techniques.

3. DATA EXTRACTION

Extraction of the spectra was performed using a custom Python pipeline which utilizes Source Extractor (via the sewpy wrapper), SAO's DS9, pyds9, openpyxl, pandas, TKinter, Skyfield, SciPy and Astropy in addition to common Anaconda distribution modules [10-20]. The extraction of the spectrum is done by first using Source Extractor to find the centroid of the zeroth order point source to indicate where the wavelength calibration begins. The brightness of the target reported by Source Extractor is recorded for use in lightcurve generation. An extraction box of user-defined dimensions is drawn around the spectrum and zeroth order point source and the wavelength is calculated as the number of pixels from the centroid of the zeroth order point source times the spectral resolution of the system. For each wavelength unit (i.e. each pixel), the number of counts in a column the height of the extraction box is determined. This is performed for all pixels within the width of the extraction box to generate a single flux vs. wavelength profile. A background estimation box of the same dimensions as the extraction box is created at a user-defined distance from the extraction box. The median number of counts from all pixels within the background estimation box is taken so that the estimation is more robust against star contamination and hot pixels. This median background value is multiplied by the number of pixels in a column of the extraction box and subtracted from the number of counts in each column of the extraction box. Finally, each spectrum is normalized to a user-defined wavelength. This process is done for all solar analog images and the results are median combined to make a master solar analog spectrum for the night. The extraction is performed on each individual target image, but with the additional step of dividing each wavelength's normalized flux by the median solar analog spectrum's value to produce a reflectance spectrum. The reflectance, wavelength, and brightness from Source Extractor are recorded along with the time since the first image and the longitudinal phase angle (LPA). Longitudinal phase angle, the East-West component of the sun-target-observer angle, is estimated using the difference between the right ascension (RA) of the target and the RA of the anti-solar point of the sun (both in degrees) such that the start of the night has negative LPA and the end of the night has positive LPA while local midnight has near-zero LPA. A second custom Python script is responsible for reading in the recorded data and plotting the desired visualizations.

4. INITIAL RESULTS

Although it is not the primary data product, a lightcurve is generated using the brightness values of the zeroth order point source and the estimated LPA, such as that seen in Fig 1. The brightness value returned is a number of

background corrected counts from the point source. The instrumental magnitude for this is calculated using the equation m_{inst} = -2.5*$\log_{10}$(counts/exposure time). A one-time estimate of the zero point was performed by simultaneous observing with RAPTORS I and the LEO-20 telescope, which uses an in-frame photometry calibration pipeline. The zero point magnitude was the shift in magnitude to make the RAPTORS instrumental magnitude match the calibrated Sloan g' filter magnitude from LEO-20. The reported "nominal g' magnitude" in Fig 1 is the calculated m_{inst} plus this estimated zero point magnitude and is intended to be used for qualitative purposes only.

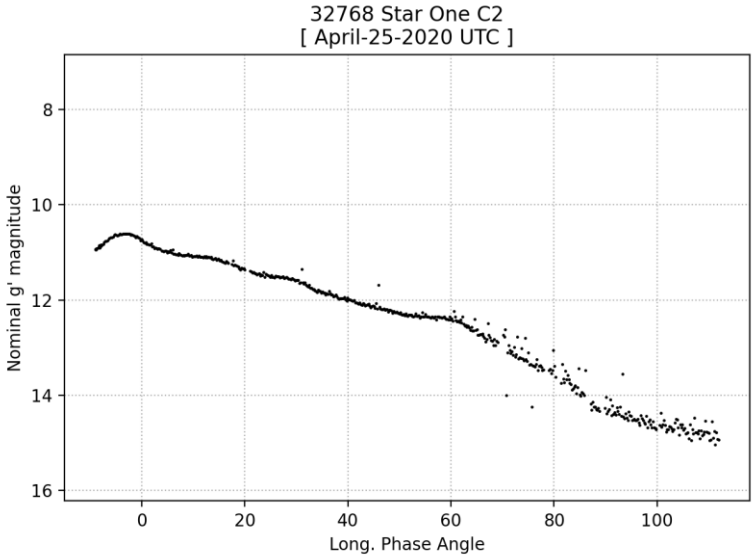

Fig 1. Lightcurve for Star One C2 (32768) showing nominal brightness vs LPA (degrees) for April 25, 2020 UTC. Stray data points that lie above and below the curve are likely due to star streaks or wind. Brightness values are not photometrically calibrated because this plot is for qualitatively showing feature locations in LPA-space.

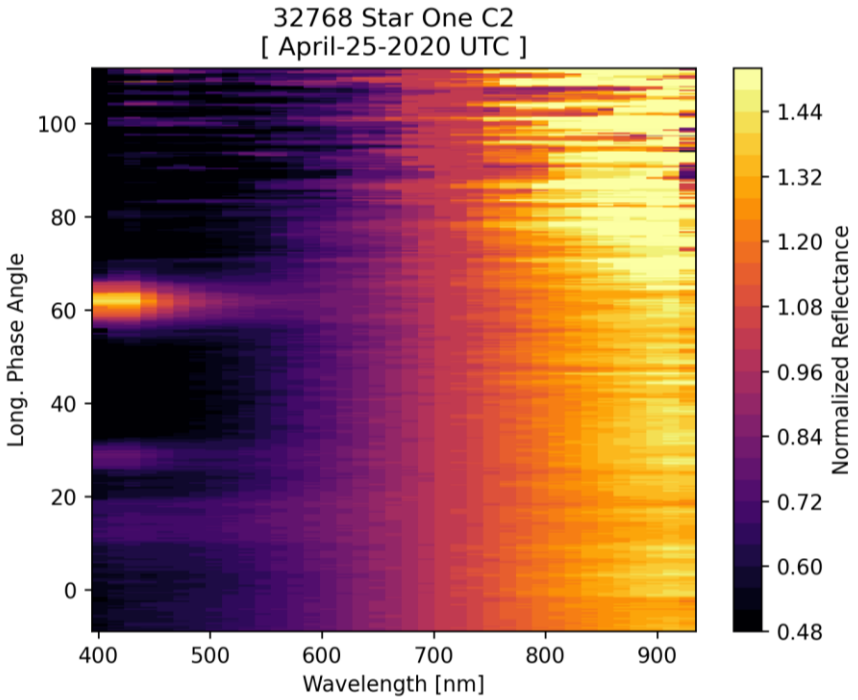

Fig 2. Spectral Phase Map of GEO Star One C2 (32768) observed on April 25, 2020 UTC showing LPA (degrees) versus wavelength (nm) with the out-of-plane axis being the normalized reflectance (700 nm = 1). Each horizontal slice across the SPM is an individual spectrum from the night of observations. The spectra are smoothed with a median kernel to bin small sets of spectra and make the image more readable.

In order to visualize the hundreds of spectra in a given night, a spectral phase map (SPM) is generated which shows the wavelength along the x-axis, LPA along the y-axis, and normalized reflectance along the z-axis (out of plane). A small (i.e. 1-7 sized) median filter smoothing kernel is applied to make the SPM more readable, suppress noise, and allow the binning of spectra. These SPMs, such as Fig 2, compress the full night of spectra into one unique image which can be used for characterization and fingerprinting of the RSO. Each horizontal slice in the SPM represents a single spectrum from the night. Spectral phase maps show feature consistency with more traditional lightcurve techniques, such as Fig 1. For most nights of data, this can most easily be seen at the zero LPA peak in the lightcurve. Additional features can sometimes be seen at LPAs where there is no obvious feature in the lightcurve. These "flux neutral" features roughly maintain the brightness of the target or the brightness trend, but shift the reflectance in wavelength space such that a new feature is seen in the SPM.

Another visualization of the data is to take the median of all the reflectance values for each wavelength across all LPA. This creates a single, full night median spectrum which can be used to represent the night of observations, as shown in Fig 3 for two objects. To represent the phase variations, the inner quartile range (IQR) is shown with the uncertainty bars on the scatter plot. This is not a representation of the error, but the range of reflectance values which captures the inner 50% of the night's reflectance variation and is chosen as a non-parametric analysis for the data. This choice of a non-parametric analysis will allow more accurate discussions of the interpretation of the results in the future. In Fig 3, for example, we can see that the spectra fall within each other's IQR at redder wavelengths, but the IQRs are separated at bluer wavelengths (i.e. short of ~650 nm). The analysis of several full night median spectra led to a hypothesis that objects of the same bus type will have similar full night spectra. The reasoning being that, throughout the full night, spectra will receive varying amounts of reflected light from the sun-tracking solar panels and the glinting payload. The diffuse, nadir pointing bus will provide more constant reflection which will dominate when the spectra are median combined across all LPA. This hypothesis will be further explored in future work, but has the potential to lead to a bus-type based GEO satellite taxonomy, similar to spectroscopy-based taxonomies used in asteroid science for object classification [21].

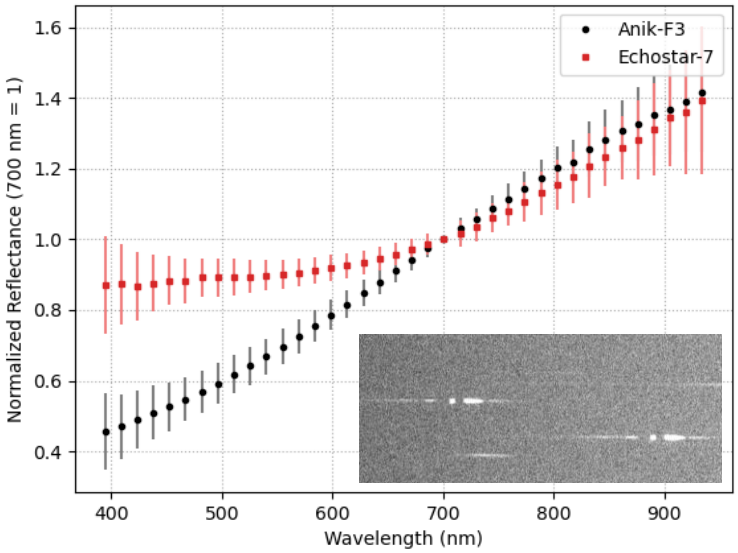

Fig 3. Comparison of full night median spectra of Anik F3 (31102) and Echostar 7 (27378). Both objects were in the same field of view for the entire night (see inset image). In the inset image, Anik F3 is left and Echostar 7 is on the right. Vertical bars here represent the IQR of LPA-induced reflectance variation for the full night of spectra.

5. ONGOING WORK

The initial results from the RAPTORS I survey have shown that low-resolution visible spectroscopy can produce several data products that help to characterize and identify GEOs. Future work will focus on completing the survey of all near-zero inclination GEOs visible from Tucson, Az., USA as well as a more in-depth study of different satellite bus types. Three satellites in each of four bus types were chosen for a total of twelve targets for the bus-type study. Objects were chosen that were as close to the local meridian as possible and all satellites of a given bus type were separated by no more than 15 degrees in orbital longitude to reduce viewing condition differences between members of the same bus type. These twelve objects will be observed once every month, if possible. Objects of the

same bus type will be observed in succession and all objects will be observed in the same order each month to reduce seasonal variations between objects of the same type. The goal of this work is to better understand seasonal variations for individual satellites and to understand if bus type is the primary factor governing an object's median spectrum. Results from this study will help determine if a bus-type based taxonomy for GEO satellite classification is possible. Once collected, this vast data set of GEO visible spectroscopy will be used to train deep learning machine algorithms for more complex analysis of the data and the development of models for predicting characteristics of GEOs based on a limited number of spectra. Once initial analyses are complete, our intention is to make the raw spectroscopy data available to other researchers in the field.

6. ACKNOWLEDGEMENTS

This work is supported in part by the cooperative agreement (FA9451-18-2-0105) between the United States Air Force Research Lab (AFRL) and the University of Arizona (PI: Prof. Roberto Furfaro) and the state of Arizona Technology Research Initiative Fund (TRIF) grant (PI: Prof. Vishnu Reddy).

7. REFERENCES

[1] Jorgensen, K., "Using Reflectance Spectroscopy to Determine Material Type of Orbital Debris," Ph.D. Thesis, Colorado Center for Astrodynamics Research, Univ. of Colorado, Boulder, CO, 2000.

[2] Jorgensen, K., Africano, J., Hamada, K., Sydney, P., Stansbery, E., Kervin, P., Nishimoto, D., Okada, J.,Thumm, T., and Jarvis, K., "Using AMOS Telescope for Low Resolution Spectroscopy to Determine the Material Type of LEO and GEO Objects," AMOS Technologies Conference, Maui Economic Development Board, Kihei, Maui, HI, Sept. 2001, pp. 127–134.

[3] Jorgensen, K., Stansbery, G., Africano, J., Hamada, K., Sydney, P., and Kervin, P., "Most recent findings from the NASA AMOS Spectral Study (NASS): Squiggly Lines Lead to Physical Properties of Orbiting Objects," AMOS Technologies Conference, Maui Economic Development Board, Kihei, Maui, HI, Sept. 2002

[4] Jorgensen, K., Okada, J., Bradford, L., Hall, D., Africano, J., Hamada, K., Sydney, P., Stansbery, G., and Kervin, P., "Obtaining Material Type of Orbiting Objects Through Reflectance Spectroscopy Measurements," AMOS Technologies Conference, Maui Economic Development Board, Kihei, Maui, HI, Sept. 2003.

[5] Abercromby, K., Okada, J., Guyote, M., Hamada, K., and Barker, E., "Comparisons of Ground Truth and Remote Spectral Measurements of the FORMOSAT and ANDE Spacecraft," AMOS Technologies Conference, Curran Associates, Redhook, NY, Sept. 2006.

[6] Reddy, V., Linder, T., Linares, R., Furfaro, R., Tucker, S., and Campbell, T., "RAPTORS: Hyperspectral Survey of the GEO Belt," AMOS Technologies Conference, Maui Economic Development Board, Kihei, Maui, HI, Sept. 2018

[7] Payne, T. E., Gregory S. A., and Luu K., "SSA Analysis of GEOS Photometric Signature Classifications and Solar Panel Offsets," AMOS Technologies Conference, Maui Economic Development Board, Kihei, Maui, HI, Sept. 2006.

[8] Harrison, K., "Prisms, Gratings, and Spectroscopes" in *Astronomical Spectroscopy for Amateurs*, 1st ed. New York, NY, USA: Springer, 2011, ch. 4, pp. 42-44.

[9] Bus, S. and Binzel, R. P., Small Main-belt Asteroid Spectroscopic Survey, Phase II. EAR-A-I0028-4-SBN0001/SMASSII-V1.0. NASA Planetary Data System, 2003.

[10] Smithsonian Astrophysical Observatory, "SAOImage DS9: A utility for displaying astronomical images in the X11 window environment", *Astrophysics Source Code Library*, 2000. ascl:0003.002.

[11] Astropy Collaboration, "Astropy: A community Python package for astronomy", *Astronomy and Astrophysics*, vol. 558, 2013. doi:10.1051/0004-6361/201322068.

[12] Astropy Collaboration, "The Astropy Project: Building an Open-science Project and Status of the v2.0 Core Package", *The Astronomical Journal*, vol. 156, no. 3, 2018. doi:10.3847/1538-3881/aabc4f.

[13] McKinney, W., "Data Structures for Statistical Computing in Python", Proceedings of the 9th *Python in Science Conference*, 51-56 (2010).

[14] Virtanen, P., Gommers, R., Oliphant, T.E., et al., and SciPy 1.0 Contributors, "SciPy 1.0: Fundamental Algorithms for Scientific Computing in Python". *Nature Methods*, 17(3), 261-272, (2020).

[15] Anaconda Software Distribution. Computer software. Vers. 2-2.4.0. Anaconda, Nov. 2016. Web, https://anaconda.com

[16] Bertin, E. and Arnouts, S., "SExtractor: Software for source extraction," *Astronomy & Astrophysics Supplement*, 317, 393, (1996).

[17] Rhodes, B. "Skyfield: Generate high precision research-grade positions for stars, planets, moons, and Earth satellites," *Astrophysics Source Code Library*, 2019. ascl:1907.024
[18] Mandel, E., PyDS9 [Software], 2020. Web. https://github.com/ericmandel/pyds9
[19] MegaLUT Developers, SewPy [Software], 2017. Web. https://github.com/megalut/sewpy
[20] Gazoni, E., and Clark, C., Openpyxl [Software], 2021. Web. https://foss.heptapod.net/openpyxl/openpyxl
[21] DeMeo, F.E., Binzel, R.P., Slivan, S.M., and Bus, S.J., 2009. An Extension of the Bus Asteroid Taxonomy into the Near-Infrared. Icarus 202, pp. 160-180.